Journal of Hazardous Materials 184 (2010) 432–438

Contents lists available at ScienceDirect

Journal of Hazardous Materials

journal homepage: www.elsevier.com/locate/jhazmat

Effect of structural variations on sorption and desorption of phenanthrene by sediment organic matter

Jinghuan Zhang[a,b], Mengchang He[a,*]

[a] State Key Laboratory of Water Environment Simulation, School of Environment, Beijing Normal University, Beijing 100875, China
[b] Department of Analytical Chemistry, China Pharmaceutical University, Nanjing 211198, China

ARTICLE INFO

Article history:
Received 6 April 2010
Received in revised form 30 August 2010
Accepted 31 August 2010
Available online 15 September 2010

Keywords:
Sediment organic matter
Black carbon
Phenanthrene
Sorption
Desorption

ABSTRACT

Sorption and desorption isotherms of phenanthrene (PHE) on sediment organic matter (SOM) prepared at different combustion temperature were studied to examine the impact of SOM structure on sorption and desorption. With the increase of combustion temperature from 0 to 400 °C, the aromatic groups (–C═C) in SOM samples increased, while the aliphatic groups (–CH, $–CH_2$) and polar structures (–C–O, –OH) decreased. When the combustion temperature increased to 500 °C, aliphatic structures, polar structures and most aromatic structures were burnt out, and the mineral materials were dominant in the sample. The increase of combustion temperature decrease the sorption isotherm nonlinearity index n value, and enhanced the adsorption capacity and desorption hysteresis for PHE on SOM. However, higher n value, lower sorption capacity and sorption irreversibility were presented in the sample treated at 500 °C (T500). Positive correlations between single-point organic carbon-normalized distribution coefficient log K_{oc} values and aromatic carbon ($p < 0.01$) and negative correlations between log K_{oc} values and aliphaticity or H/C ratios ($p < 0.05$) were observed. There was a negative relation between hysteresis index (HI) value and aromatic carbon ($p < 0.01$) and a negative trend of the sorption isotherm nonlinearity index n values and aromatic carbon ($p < 0.01$). The above results indicated the dominance of aromatic structures in the sorption nonlinearity, sorption capacity and desorption hysteresis of PHE on SOM.

1. Introduction

Hydrophobic organic compounds (HOCs) are of specific concern due to their toxic, mutagenic and highly carcinogenic properties and also due to the continuous release in the environment through natural processes and human activities. Sorption and desorption of HOCs are major processes determining the distribution, transport, bioavailability and toxicity of these compounds in soils and sediments. Soil/sediment organic matter (SOM) was considered to be the predominant sorbent for HOCs in natural environments [1,2]. It has been reported that SOM comprises two important heterogeneous sorption domains: a "soft" or amorphous domain, including fulvic acids (FAs) and humic acids (HAs) in their rubbery states, and a "hard" or condensed domain, including kerogen, coal, black carbon (BC) and HAs in their glassy states. The soft SOM domain is characterized by linear sorption isotherms, relatively rapid rates of sorption and desorption, and little or no sorption–desorption hysteresis of sorbed HOCs. Conversely, the hard SOM domain is possibly responsible for nonlinear sorption isotherms, slow rates of sorption and desorption and significant sorption–desorption hysteresis of sorbed HOCs [3–5].

Different sources result in different structures in SOM, including–COOH, –OH, –C–O, –C═O, –C═C, –C–H, etc. These structures result in different SOM properties, such as polarity, aromatic and aliphatic carbons, H/C ratios, and therefore, had different impacts on the sorption and desorption behavior of HOCs [6–9]. Xing reported that HOCs sorption nonlinearity increased with the increasing aromaticity of the HAs from soil [10]. The increase of aromatic carbon enhanced the sorption capacity of HOC on SOM [11,12], but was inversely proportional to the polarity ((N + O)/C) of SOM from different soil and sediments [6]. Furthermore, a number of studies have showed the differences of the sorption behavior of HOCs on charcoals, prepared at different temperatures, from grass or wood [13–15]. However, little information is available about the effects of structural variations of SOM on the desorption behavior of PHE. And the dependency of sorption and desorption mechanisms for PHE onto SOM with different structures, is poorly understood.

In this study, eight SOM samples with various structures and compositions were prepared by being combusted at 0, 175, 225, 275, 325, 375, 400 and 500 °C, respectively. The aims of this study were to (1) characterize the SOM samples prepared at different combustion temperatures; (2) examine the sorption and desorp-

* Corresponding author. Tel.: +86 10 58807172; fax: +86 10 58807172.
E-mail address: hemc@bnu.edu.cn (M. He).

0304-3894/$ – see front matter © 2010 Elsevier B.V. All rights reserved.
doi:10.1016/j.jhazmat.2010.08.123

tion of PHE on these SOM samples; (3) explore the effects of structural and compositional variations of SOM on PHE sorption and desorption. Our results may be useful for understanding the effects of structural variations on the transport and fate of HOCs in soils and sediments.

2. Materials and methods

2.1. Sorbent preparation and characterization

One surface (0–20 cm) sediment sample was collected from the Taizihe River in Daliaohe River water system, NE China, in May 2006. After collection, the sediment was kept frozen at −20 °C before analysis. Frozen aliquots of the sediment were freeze dried by freeze drier (FD-1A, China), passed through a 100-mesh sieve and stored in brown glass bottles. The sample was treated with the method reported by Ran et al. [27]. Firstly, carbonates in the sediment were dissolved in 1 M HCl for 24 h. Then, the residues were demineralized with 1 M HCl and 10% HF for 5 days, which was repeated four times. Finally, the residual fraction was heated in a muffle furnace at 0, 175, 225, 275, 325, 375, 400 and 500 °C for 24 h under a constant air flow of 200 mL/min to obtain SOM samples (T0, T175, T225, T275, T325, T375, T400, T500) with different surface structure. The samples were washed with deionized water, freeze-dried, gently ground to pass though a 100-mesh sieve, and stored for subsequent use. The elemental compositions (C, H, N, O) of the samples were analyzed with a high-temperature combustion method (elementar Vario EL, Germany). Ash content was determined by combustion at 740 °C for 4 h. The FTIR spectra were recorded in the transmission mode by a NEXUS 670X spectrophotometer using KBr pellet. The ^{13}C NMR spectra were acquired on a Bruker AU-300 spectrometer using cross-polarization magic angle spinning (CPMAS) techniques. Scanning electron microscopy (SEM) analysis of the samples was performed with a microscope of Hitachi S-34800N (Japan). Prior to SEM analysis, the samples on the stubs were gold coated twice using a sputter coater.

2.2. Sorption and desorption experiments

All sorption experiments were conducted in duplicates in 50 mL glass tubes with Teflon-lined caps. The PHE (>98%, Aldrich Chemical Co.), used in the experiments, has an aqueous solubility S_w at 25 °C of 1.29 mg/L and a $\log K_{ow}$ of 4.57 [16]. Stock solutions of PHE were prepared in HPLC-grade methanol. In order to prevent varying solvent effects, the volumetric fraction of methanol in the aqueous solutions were always less than 0.2% [17]. A mixture of 0.01 M $CaCl_2$ and 200 mg/L NaN_3 was used as background solution to prevent biological degradation of PHE. The ratio water:solids was always adjusted to achieve 30–80% sorption of PHE. Ten levels of initial solutions ranging from 0.05 to 1.20 mg/L were prepared in the sorption experiments. A 7 d period was chosen, since previous studies revealed it as the time necessary to reach the equilibrium. Reactors were filled with sorbent that was completely mixed with 40 mL of an initial aqueous solution by shaking at 25 ± 0.5 °C for 7 d. After centrifugation at 4000 rpm for 20 min, The PHE in the supernatant solution was determined by high performance liquid chromatograph (HPLC). Control reactors, prepared similarly but with no sorbent, were run simultaneously for assessing loss of solute due to sorption on the reactor surface. Results showed that average system losses were consistently less than 4% of initial concentration for PHE, indicating that microbial degradation and volatilization during sorption and also the uptake by the glass walls were negligible. Hence, no correction was made during reduction of sorption data.

Desorption experiments were conducted immediately after the adsorption experiments. 20 mL of the centrifuged supernatant was removed and replaced with the same volume of fresh 0.01 M $CaCl_2$ and 200 mg/L NaN_3 solution. The mixtures were then re-equilibrated for 24 h at 25 ± 0.5 °C. The separation of the SOM phase from the aqueous phase and the subsequent analysis were conducted as described above. These steps were repeated five times consecutively.

2.3. Determination of PHE

PHE concentrations were determined using a reversed phase HPLC (C18 column, 4.6 mm × 25 mm, Waters, U.S.A.) with a fluorescence detector (model Waters 474, UV excitation/emission wavelengths at 292/366 nm). Isocratic elution was performed at a flow rate of 1.0 mL/min using methanol:water (90:10) as the mobile phase. Under such HPLC conditions PHE showed a single peak at a retention time of 5.1 min. Solid phase concentrations were calculated according to the mass balance of PHE between the water and solid phase.

2.4. Data analysis

The Freundlich isotherm model has the following form [10]:

$$q_e = K_F \cdot C_e^n \quad (1)$$

and

$$\log q_e = \log K_F + n \log C_e \quad (2)$$

K_{FOC} can be calculated from K_F:

$$K_{FOC} = \frac{K_F}{f_{oc}} \quad (3)$$

where C_e is the liquid phase equilibrium concentration in mg/L and q_e is the concentration on the solid phase in μg/g, K_F is the sorption capacity-related parameter [(μg/g)/(mg/L)^n], n is the isotherm nonlinearity index, K_{FOC} is the OC-normalized sorption parameter and f_{oc} is the organic carbon content of the sorbent (%). The concentration dependent OC-normalized sorption coefficient K_{oc} at three selected concentrations (C_e = 0.05 mg/L, C_e = 0.5 mg/L, C_e = 0.1 mg/L) was calculated based on the equation [8]:

$$K_{oc} = K_{FOC} C_e^{n-1} \quad (4)$$

The hysteresis index (*HI*) for the sorption–desorption isotherm is calculated using the formula [18]:

$$HI = \frac{n_{des}}{n_{ads}} \quad (5)$$

where n_{ads} and n_{des} are the isotherm nonlinearity index of the adsorption and desorption isotherms, respectively. The fitting was processed using SigmaPlot 2000 (SPSS Inc.) and statistical analysis was performed using SPSS 11.0 (SPSS Inc.).

3. Results and discussion

3.1. Characteristics of different SOM samples

3.1.1. Elemental analysis

The elemental composition of the SOM samples is given in Table 1. With increasing combustion temperature, the C, H, N and O content decreased from 29.1 to 0.10%, from 2.68 to 0.34%, from 0.93 to 0.10% and from 7.95 to 1.36%, respectively. The observed H/C and O/C atomic ratios also decreased. A higher H/C ratio may suggest a higher degree of aliphaticity [7]. The much higher H/C ratio for T0 and T175 (H/C ratio >1.0) suggests that the samples contain a good amount of original organic residues,

Table 1
Elemental composition of SOM samples and Feundlich sorption and desorption parameters of PHE on different SOM samples.

Sorbents	Elemental composition (%)				Sorption				Desorption				*HI*[a]
	C	H	N	O	*n*	R^2	K_{FOC}	N^b	*n*	R^2	K_{FOC}	N^b	
T0	29.1	2.68	0.93	7.95	0.643 ± 0.005[c]	0.998	27,893	20	0.365 ± 0.004[c]	0.986	22,488	12	0.57
T175	24.2	2.07	0.6	5.67	0.561 ± 0.004	0.995	28,773	20	0.275 ± 0.002	0.989	24,091	12	0.49
T225	23.4	1.41	0.54	5.46	0.521 ± 0.005	0.985	29,423	20	0.219 ± 0.003	0.980	24,406	12	0.42
T275	20.6	1.13	0.43	4.58	0.489 ± 0.003	0.990	34,709	20	0.177 ± 0.004	0.980	28,262	12	0.36
T325	17	0.83	0.27	3.42	0.460 ± 0.006	0.989	63,429	20	0.143 ± 0.003	0.981	49,653	12	0.31
T375	12.2	0.54	0.13	2.14	0.444 ± 0.003	0.994	101,959	20	0.105 ± 0.004	0.984	76,590	12	0.24
T400	8.97	0.34	0.1	1.36	0.387 ± 0.004	0.993	129,788	20	0.074 ± 0.002	0.984	90,357	12	0.19
T500	0.10	–	–	–	0.706 ± 0.009	0.982	28,750	20	0.428 ± 0.007	0.981	26,000	12	0.61

[a] *HI* is the hysteresis index.
[b] Number of data.
[c] Standard deviation.

such as polymeric CH_2 and fatty acid, lignin and some cellulose, while the H/C of 0.46 for T400 indicates a higher aromatic structure. The T375 sample termed as BC has H/C and O/C ratios of 0.53 and 0.13, close to the reported data for chars in the literature [19,20]. The decrease of the polarity index [(N + O)/C] with the combustion temperature indicates a reduction of the surface polar functional groups. The ash content was of 57.9–97.8%, increasing with the combustion temperature, which suggests relatively large mineral associations for high-temperature sample.

3.1.2. FTIR spectra analysis

The FTIR spectra for the SOM samples are shown in Fig. 1. All absorption bands experience different changes with increasing combustion temperature. For all samples, the broad band observed at about 3400 cm^{-1} is assigned to the stretching vibration of hydroxyl groups. Peaks at 2925 and 2850 cm^{-1} are ascribed to aliphatic CH_2 asymmetric and symmetric stretching, respectively [21]. The band at 1460 cm^{-1} is the deformation of aliphatic C–H [22]. The bands for aliphatic CH_2 (2925, 2850 and 1460 cm^{-1}) diminished gradually at low combustion temperature (0–225 °C) and are completely eliminated when heating to 275 °C. This observation indicates a decrease of aliphatic carbon content with increasing combustion temperature. The sharp and strong band at 1640 cm^{-1}can be assigned to aromatic C=C stretching [23]. The absorbance at 1270 cm^{-1} for T0 is the C–H stretching and OH deformation of COOH or C–O stretching of aryl esters [24] and disappeared when heating to 175 °C. The band due to aliphatic C–O–C and alcohol-OH (1190 cm^{-1}) decreased with increasing combustion temperature and disappeared at 375 °C, suggesting a reduction of polar groups (–OH and C–O). The peak at 660 cm^{-1} is associated with unknown mineral compounds.

3.1.3. CP/MAS ^{13}C NMR spectra analysis

The CP/MAS ^{13}C NMR spectra of the SOM samples are presented in Fig. 2. Within the 0–220 ppm chemical shift range, the peaks on the ^{13}C NMR spectra are assigned to alkyl-C (0–50 ppm); O-alkyl-C (50–100 ppm); aromatic-C (110–165 ppm); carboxyl-C (165–190 ppm) and carbonyl-C (190–220 ppm). Alkyl carbon and aromatic carbon are attributed to nonpolar carbons, which will contribute to adsorption of apolar organic pollutants. As shown in Fig. 2, the ^{13}C NMR spectra showed major peaks at 27 and 43 ppm (alkyl-C), 53 and 70 ppm (O-alkyl-C), 125 ppm (aromatic-C) and 170 ppm (carboxyl-C) for T0, T175, T225 and T275 and exhibited only one major peak at 123 ppm for T325, T375 and T400. This reveals a large contribution from aromatic carbon for high-temperature samples, which is comparable to biochars prepared at different temperatures [15]. The aliphatic carbon is the highest for T0 and decreased with combustion temperature, whereas the observed aromatic carbon content increased. Moreover, the aliphaticity decreased from 0.66 to 0.23, which was consistent with the reduction of H/C ratio. The carboxyl carbon and carbonyl carbon were of 4.49–10.2% and 0.78–3.60%, respectively. The observation is in line with the results of FTIR spectra and elemental composition analysis. The above results may affect the sorption capacity and nonlinearity of the sorption isotherms of PHE.

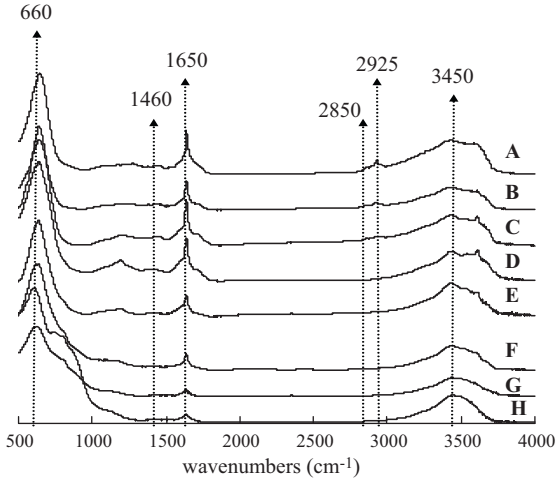

Fig. 1. FTIR spectra of different SOM samples. (A) T0; (B) T175; (C) T225; (D) T275; (E) T325; (F) T375; (G) T400; (H) T500.

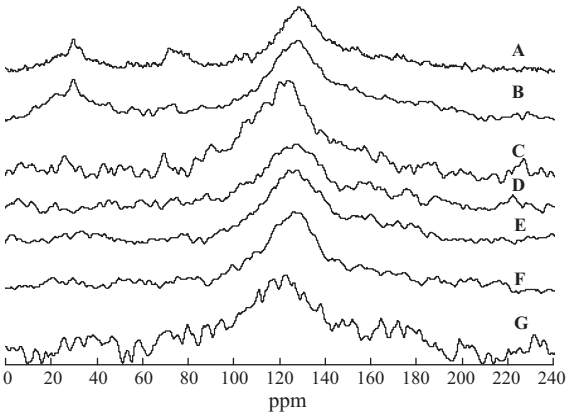

Fig. 2. CP/MAS ^{13}C NMR spectra of different SOM samples. (A) T0; (B) T175; (C) T225; (D) T275; (E) T325; (F) T375; (G) T400.

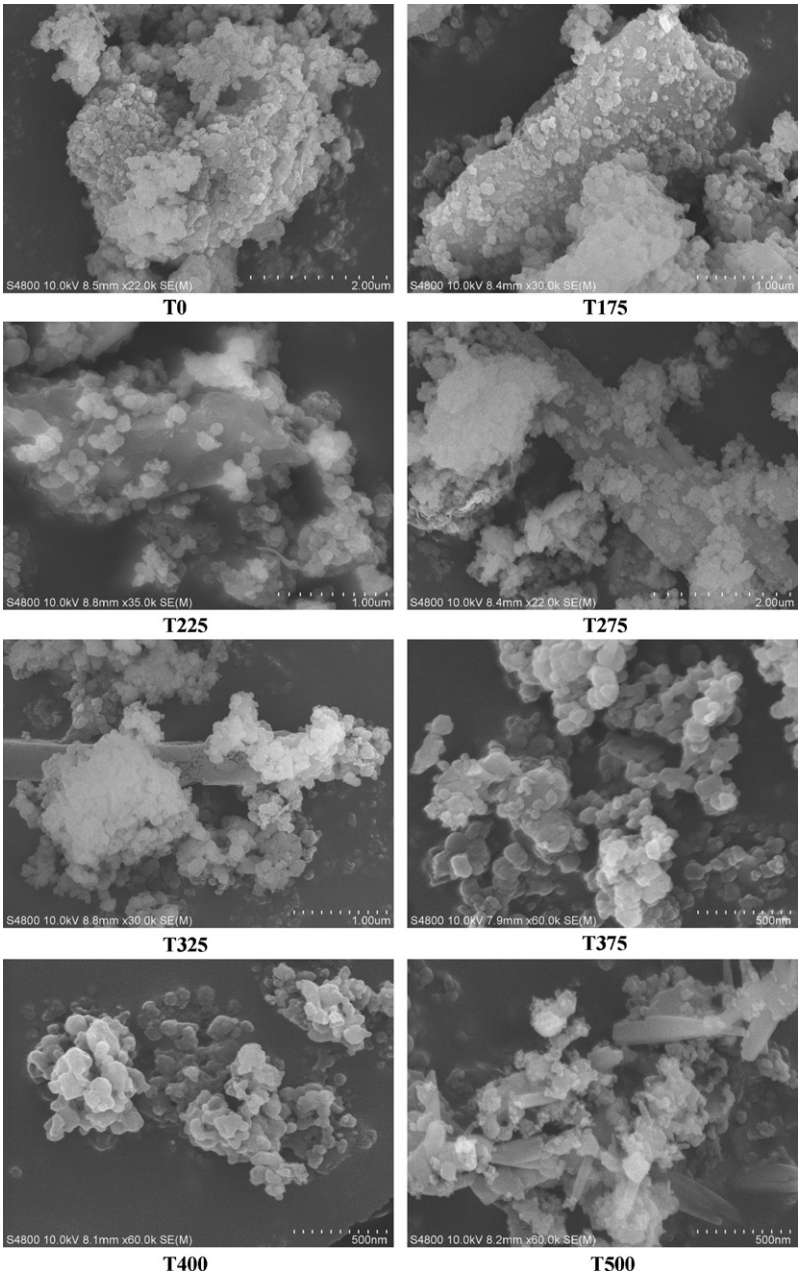

Fig. 3. SEM analysis of different SOM samples.

3.1.4. SEM analysis

The SEM analysis of SOM samples obtained at different combustion temperatures are shown in Fig. 3. Upon SEM observation, there was no significant difference in morphology between T0, T175, T225, T275 and T325 samples, and these samples had irregular shapes and rough surface with flocculent and nubby organism combined together. However, the T375 and T400 samples had unique globular and porous structures, which may result in their high specific surface area and therefore relatively high sorption affinity for organic compounds. With the increase of combustion temperature, the soft carbon structure in SOM was burnt out, and thus, the structure in T375 and T400 samples was dominated by hard carbon domain. When the combustion temperature increased to 500 °C, the globular structures were destroyed and some aggregated bacilliform structures appeared. Moreover, the image of T375 sample defined as BC material was similar to that of SRM 2975 diesel soot reported by Nguyen et al. [25].

3.2. Influence of SOM structure on the sorption of PHE

PHE sorption and desorption isotherms on SOM samples obtained at different combustion temperatures are given in Fig. 4. All sorption and desorption isotherms were nonlinear with the Freundlich parameters listed in Table 1. As shown in Table 1, the increase of combustion temperature enhanced the adsorption nonlinearity of PHE on SOM samples except the T500 sample. When the combustion temperature increased from 0 to 400 °C, the n value for SOM samples decreased from 0.643 to 0.387. However, the sorption of PHE on the T500 sample became more linear than the T0 sample with n value of 0.706. After heating at 500 °C, most organic matter was burn out and the minerals are the domain in the sample, which dominated the less nonlinear sorption of PHE. The nonlinearity factor n is related to sorption site energy distribution and is related to heterogeneous glass, hard, or condensed SOM domain and to the maturation degree of SOM [4]. The lower

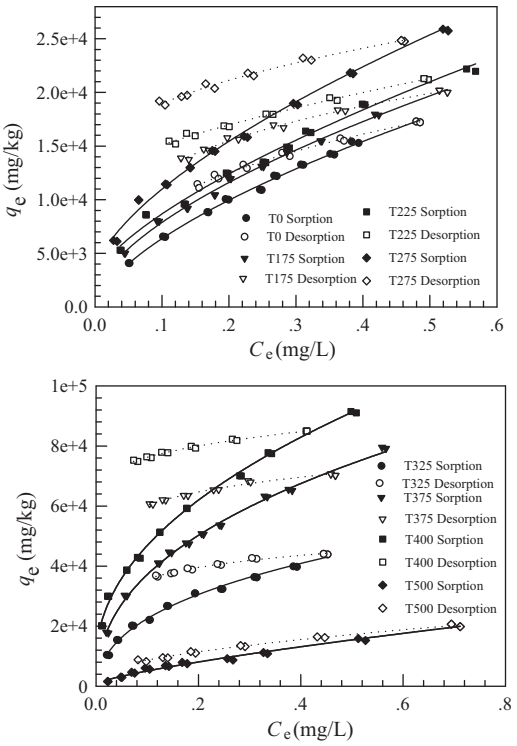

Fig. 4. Sorption and desorption isotherms of PHE on different SOM samples.

the n value is, the more heterogeneous is the sorption site energy distribution or the higher is the degree of SOM maturation [1,4]. Thus, the lower n value in the T400 sample indicates the more condensed and rigid structure and a wider distribution of sorption energy.

The $\log K_{FOC}$ values increased from 27,893 to 129,788 $(\mu g/g\,OC)/(mg/L)^n$ for the samples (T0–T400). Moreover, the concentration-dependent OC-normalized sorption coefficient value, K_{oc}, for PHE decreases as a function of C_e due to the isotherm nonlinearity. For a given C_e, the K_{oc} values increased from the T0 sample to the T400 sample, gradually. The K_{oc} values for the T400 sample were about 5.6–10.0 times higher than those for the T0 sample at a given C_e. However, the lowest K_{oc} values were presented in the T500 sample, which were even lower than those for the T0 sample. The above results indicated an increase in sorption capacity for PHE with the combustion temperature increasing from 0 to 400 °C. The difference in sorption capacity may be due to their different surface structure and composition of the SOM samples prepared at different combustion temperatures. According to the results of FTIR spectra and ^{13}C NMR spectra analysis, from T0 to T400 sample, the aliphatic carbon (–CH, $–CH_2$) decreased, while the aromatic carbon (–C=C) increased. Furthermore, there was a decrease trend in polar structures (–C–O, –OH) in the SOM samples (from T0 to T400). Thus, the higher sorption affinity for the T400 sample was attributed to the aromatic groups in the sample.

3.3. Influence of SOM structure on the desorption of PHE

The desorption isotherms, Freundlich fitting parameters and *HI* values for the desorption of PHE on the SOM samples prepared at different combustion temperature are given in Fig. 4 and Table 1. As shown in Table 1, a decrease trend in n values for PHE desorption was found with the combustion temperature increasing from 0 to 400 °C, which was similar to that for PHE sorption process. Moreover, the $\log K_{FOC}$ values in the SOM samples (from T0 to T400) increased from 22,488 to 90,357 $(\mu g/g\,OC)/(mg/L)^n$. The value of *HI* reflects the sorption irreversibility of PHE on the SOM samples. In general, a value of *HI* close to 1 indicates that desorption process performs as quickly as sorption does, thus, the sorption is reversible. While a value of $HI < 1$ reveals that the rate of desorption is lower than that of sorption, therefore, hysteresis takes place [26]. In this study, the desorption of PHE from different SOM samples was hysteretic with *HI* values of 0.19–0.61. The increase of combustion temperature strongly enhanced the desorption hysteresis of PHE on the SOM samples. When the combustion temperature increased from 0 to 400 °C, the *HI* value decreased from 0.57 to 0.19. This suggests that the sorbed PHE in the T400 sample was highly irreversible, which may be due to its higher content of aromatic groups (–C=C). However, when the combustion temperature increased to 500 °C, the desorption of PHE was prompted with *HI* value increasing to 0.61. This may be attributed to the mineral materials in the T500 sample. Thus, we can conclude that the SOM sample with more aromatic structure had higher sorption capacity and sorption irreversibility of PHE, therefore, effectively making PHE immobile in the environment. But the sample with more aliphatic carbon exhibited lower sorption capacity and higher sorption reversibility of PHE. Thus, it may mobilize PHE by removing sorbed PHE to aqueous phase in contaminated soils and sediments.

3.4. Correlations of PHE sorption and desorption parameters with SOM properties

Correlations of Freundlich sorption and desorption parameters with SOM properties are given in Fig. 5. Application of ^{13}C NMR spectra and elemental composition analysis facilitates the exploration of the relationship between the structural characteristics and Freundlich isotherm sorption and desorption parameters, K_{oc}, n and *HI* values. As shown in Fig. 5, there was a negative relation between n values and aromatic carbon ($p < 0.01$) and a positive correlation of n values and aliphaticity ($p < 0.01$) or H/C ratios ($p < 0.01$), which indicated that higher aromatic carbon content in SOM resulted in lower n value, and thus revealing the importance of aromatic structures in PHE sorption nonlinearity. This is similar to the results in the literature [27]. But a different conclusion was observed for the sorption of PHE and benzo[α]pyrene to HAs [28,29]. Positive correlations between $\log K_{oc}$ values at each of the three concentrations and aromatic carbon for the SOM samples were observed ($p < 0.01$), revealing the importance of the aromatic groups on K_{oc}. However, there were negative correlations between $\log K_{oc}$ values at the three PHE concentrations and aliphaticity or H/C ratios, respectively ($p < 0.05$). This is different from the results of Kang and Xing [7]. But Grathwohl reported that old and relatively high aromatic organic matter found in shale or coal had higher K_{oc} values than younger organic matter obtained from a surface soil [11]. A similar conclusion was also observed by Xu et al. [12]. Our results were agreement with known report and further showed that the SOM samples with high aromatic carbon or low H/C ratios or aliphaticity exhibited stronger and more nonlinear sorption for PHE. In addition, a negative relation of *HI* value and aromatic carbon ($p < 0.01$) and a positive correlations between *HI* value and aliphaticity ($p < 0.01$) were found. This indicated that the increase of aromatic carbon in SOM enhanced the sorption irreversibility of PHE, thus, preventing the mobility of PHE in the environment. The above results suggested the dominant role of aromatic carbon in the sorption nonlinearity, sorption capacity and desorption hysteresis of PHE on SOM.

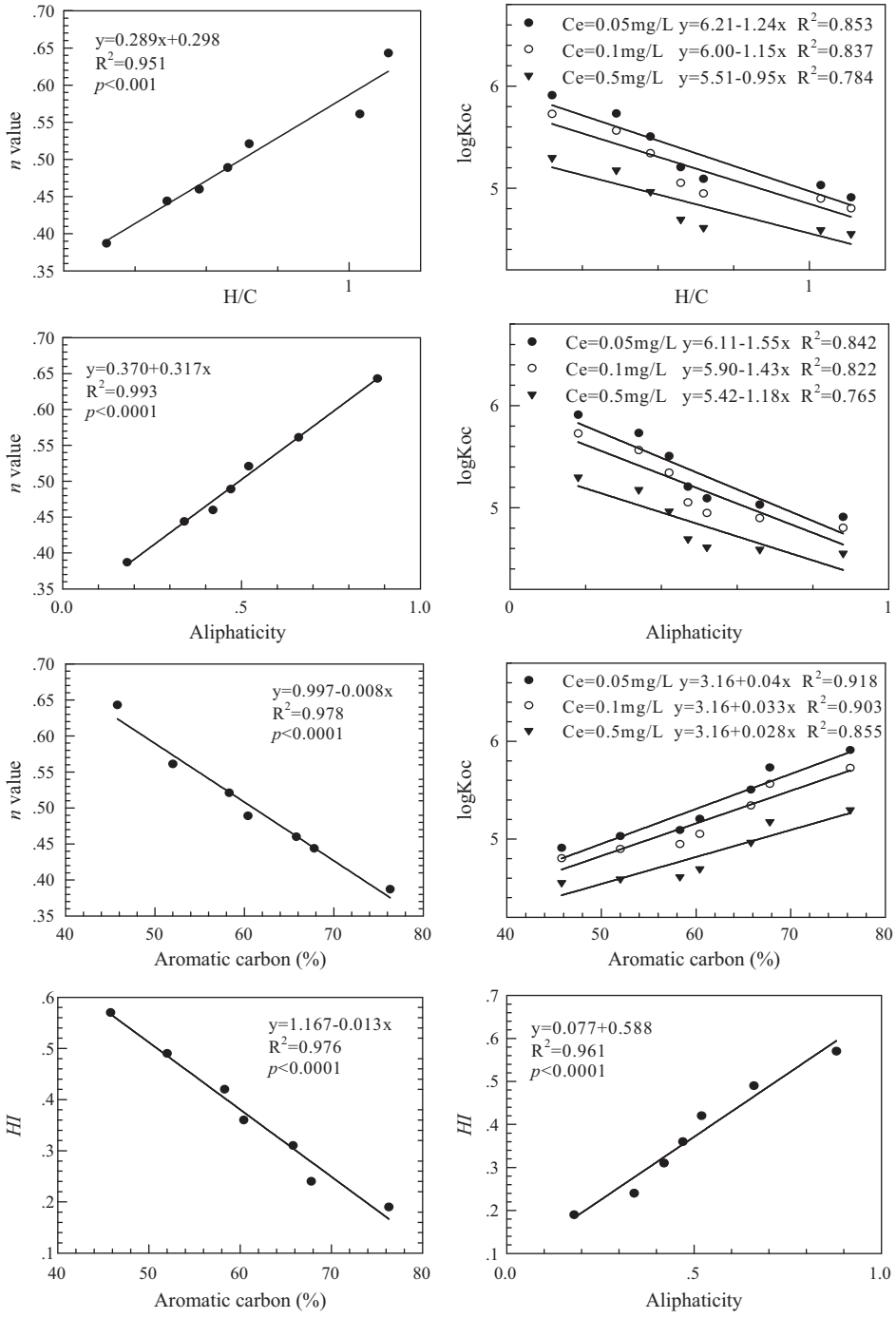

Fig. 5. Correlations of PHE sorption and desorption parameters with SOM properties.

4. Conclusions

The increase of combustion temperature resulted in an increase of aromatic groups (–C=C), and a reduction of aliphatic groups (–CH, $–CH_2$) and polar structures (–C–O, –OH) in SOM samples, therefore, leading to the difference in sorption nonlinearity, sorption affinity and reversibility for PHE. With the combustion temperature increasing from 0 to 400 °C, the adsorption nonlinearity, desorption nonlinearity, desorption hysteresis and K_{oc} values for PHE at a given C_e increased, gradually. However, when the combustion temperature increased to 500 °C, more linear sorption, lower sorption capacity and sorption irreversibility were observed, which may be due to the mineral materials in the T500 sample. Positive relations of log K_{oc} values at the three PHE concentrations and aromatic carbon in SOM ($p < 0.01$), a negative correlation between *HI* value and aromatic carbon ($p < 0.01$) and a negative trend of *n* values and aromatic carbon ($p < 0.01$) were found, indicating the dominance of aromatic structures in sorption nonlinearity, sorption capacity and irreversibility of PHE on SOM. Our findings may be helpful for understanding the distribution, transport and fate of HOCs in soils and sediments.

Acknowledgments

The study was jointly supported by the project of National Basic Research Program of China (Grant No. 2004CB418502), the pro-

gram for Changjiang Scholars and Innovative Research Team in University (No. IRT0809), the Scientific Research Foundation of Beijing Normal University (No. 2009SD-8) and special fund of State Key Laboratory of Water Environment Simulation (No. 08ESPCT-Z).

References

[1] J.J. Pignatello, Soil organic matter as a nanoporous sorbent of organic pollutants, Adv. Colloid Interface Sci. 76/77 (1998) 445–467.
[2] K. Yang, L. Zhu, B. Lou, B. Chen, Correlations of nonlinear sorption of organic solutes with soil/sediment physicochemical properties, Chemosphere 61 (2005) 116–128.
[3] E.J. LeBoeuf, W.J. Weber Jr., A distributed reactivity model for sorption by soils and sediments. 8. Sorbent organic domains: discovery of a humic acid glass transition and an argument for a polymer-based mode, Environ. Sci. Technol. 31 (1997) 1697–1702.
[4] W.J. Weber Jr., P.M. McGinley, L.E. Katz, A distributed reactivity model for sorption by soils and sediments. 1. Conceptual basis and equilibrium assessments, Environ. Sci. Technol. 26 (1992) 1955–1962.
[5] T.M. Young, W.J. Weber Jr., A distributed reactivity model for sorption by soils and sediments. 3. Effects of diagenetic processes on sorption energetics, Environ. Sci. Technol. 29 (1995) 92–97.
[6] B. Xing, The effect of the quality of soil organic matter on sorption of naphthalene, Chemosphere 35 (1997) 633–642.
[7] S. Kang, B. Xing, Phenanthrene sorption to sequentially extracted soil humic acids and humins, Environ. Sci. Technol. 39 (2005) 134–140.
[8] B. Wen, J. Zhang, S. Zhang, X. Shan, S.U. Kuan, B. Xing, Phenanthrene sorption to soil humic acid and different humin fractions, Environ. Sci. Technol. 41 (2007) 3165–3171.
[9] J. Trickovic, I. Ivancev-Tumbas, B. Dalmacija, A. Nikolic, S. Trifunovic, Pentachlorobenzene sorption onto sediment organic matter, Org. Geochem. 38 (2007) 1757–1769.
[10] B. Xing, Sorption of naphthalene and phenanthrene by soil humic acids, Environ. Pollut. 111 (2001) 303–309.
[11] P. Grathwohl, Influence of organic matter from soils and sediments from various origins on the sorption of some chlorinated aliphatic hydrocarbons: implications on K_{oc} correlations, Environ. Sci. Technol. 24 (1990) 1687–1693.
[12] D. Xu, S. Zhu, H. Chen, F. Li, Structural characterization of humic acids isolated from typical soils in China and their adsorption characteristics to phenanthrene, Colloids Surf. A 276 (2006) 1–7.
[13] G. James, D.A. Sabatini, C.T. Chiou, D. Rutherford, A.C. Scott, H.K. Karapanagioti, Evaluating PHEanthrene sorption on various wood chars, Water Res. 39 (2005) 549–558.
[14] L. Bornemann, R. Kookana, G. Welp, Differential sorption behavior of aromatic hydrocarbons on charcoals prepared at different temperatures from grass and wood, Chemosphere 67 (2007) 1033–1042.
[15] B. Chen, D. Zhou, L. Zhu, Transitional adsorption and partition of nonpolar and polar aromatic contaminants by biochars of pine needles with different pyrolytic temperatures, Environ. Sci. Technol. 42 (2008) 5137–5143.
[16] D. Mackay, W.Y. Shiu, K.C. Ma, Illustrated Handbook of Physical–Chemical Properties and Environmental Fate for Organic Chemicals, vols. 1–2, Lewis Publishers, Chelsea, 1992.
[17] R.D. Wauchope, W.C. Koskinen, Adsorption–desorption equilibria of herbicides in soil: a thermodynamic perspective, Weed Sci. 31 (1983) 504–512.
[18] E. Barriuso, D.A. Laird, W.C. Koskinen, R.H. Dowdy, Atrazine desorption from smecties, Soil Sci. Soc. Am. J. 58 (1994) 1632–1638.
[19] J. Song, P. Peng, W. Huang, Black carbon and kerogen in soils and sediments. 1. Quantification and characterization, Environ. Sci. Technol. 36 (2002) 3960–3967.
[20] X. Wang, T. Sato, B. Xing, Competitive sorption of pyrene on wood chars, Environ. Sci. Technol. 40 (2006) 3267–3272.
[21] E.B.H. Santos, A.C. Duarte, The influence of pulp and paper mill effluents on the composition of the humic fraction of aquatic organic matter, Water Res. 32 (1998) 597–608.
[22] N. Senesi, V. D'Orazio, G. Rice, Humic acids in the first generation of Eurosoils, Geoderma 116 (2003) 325–344.
[23] J. Niemeyer, J. Chen, J.M. Bollag, Characterization of humic acids, composts, and peat by diffuse reflectance Fourier transform infrared spectroscopy, Soil Sci. Soc. Am. J. 56 (1992) 135–140.
[24] Y. Chun, G. Sheng, C.T. Chiou, Evaluation of current techniques for isolation of chars as natural adsorbents, Environ. Sci. Technol. 38 (2004) 4227–4232.
[25] T.H. Nguyen, R. Brown, W.P. Ball, An evaluation of thermal resistance as a measure of black carbon content in diesel soot, wood char, and sediment, Org. Geochem. 35 (2004) 217–234.
[26] A. Pusino, V.W. Pinna, C. Gessa, Azimsulfuron sorption–desorption on soil, J. Agric. Food Chem. 52 (2004) 3462–3466.
[27] Y. Ran, K. Sun, Y. Yang, B. Xing, A. Zeng, Strong sorption of PHEanthrene by condensed organic matter in soils and sediments, Environ. Sci. Technol. 41 (2007) 3952–3958.
[28] J. Zhang, M. He, H. Deng, Comparative sorption of PHEanthrene and benzo[α]phrene to soil humic acids, Soil Sedim. Contam.: Int. J. 18 (2009) 725–738.
[29] J. Zhang, M. He, Y. Shi, Comparative sorption of benzo[α]phrene to different humic acids and humin in sediments, J. Hazard. Mater. 166 (2009) 802–809.